Journal of Medicinal Chemistry

Article

pubs.acs.org/jmc

High DNA Affinity of a Series of Peptide Linked Diaromatic Guanidinium-like Derivatives

Padraic S. Nagle,[†] Fernando Rodriguez,[†,§] Binh Nguyen,[‡,∥] W. David Wilson,[‡] and Isabel Rozas*[,†]

[†]School of Chemistry, Trinity Biomedical Sciences Institute, University of Dublin, Trinity College, Pearse St., Dublin 2, Ireland

[‡]Department of Chemistry, Georgia State University, Atlanta, Georgia, United States

Supporting Information

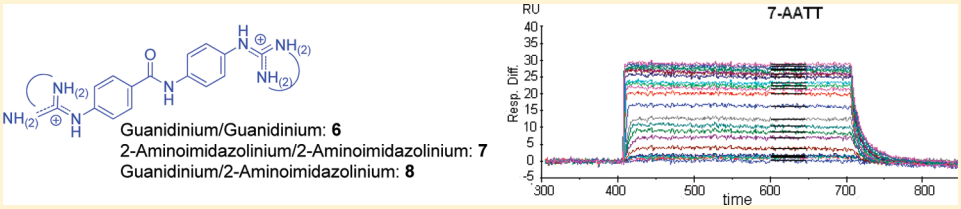

ABSTRACT: In this paper we report the design and synthesis of a new family of asymmetric peptide linked diaromatic dications as potent DNA minor groove binders. These peptide-linked compounds, with a linear core, displayed a much larger affinity than other guanidinium-like derivatives from the same series with curved cores. As a first screening, the DNA affinity of these structures was evaluated by means of thermal denaturation experiments, finding that the nature of the cation (guanidinium vs 2-aminoimidazolinium) significantly influenced the binding strength. Their binding affinity was assessed by implementing further biophysical measurements such as surface plasmon resonance and circular dichroism. In particular, it was observed that compounds **6**, **7**, and **8** displayed both a strong binding affinity and significant selectivity for AT oligonucleotides. In addition, the thermodynamics of their binding was evaluated using isothermal titration calorimetry, indicating that the binding is derived from favorable enthalpic and entropic contributions.

INTRODUCTION

The DNA minor groove is an important target site for many synthetic compounds, and for that reason, during the past 5 years, we have been designing and preparing symmetric and asymmetric bis-cationic diaromatic derivatives as DNA minor groove binders. Thus, we have been able to develop new molecular species with good affinity toward DNA and the ability to recognize specific sequences.[1−3]

Minor groove binders are finding application in different biological fields. Thus, a correlation between DNA binding affinity at AT sites and trypanocidal activity for a series of derivatives was found, supporting the hypothesis that the antitrypanosomal activity could occur by the formation of a DNA complex.[4] In this sense, a number of bis(2-amino-imidazolinium) diaromatic derivatives that bind strongly to the DNA minor groove have been reported by Dardonville, Rozas, and co-workers with very good antitrypanosomal and anti-plasmodial activity.[3] In addition, Motoshima et al. have reported a series of bis-amide derivatives related to furamidine that show very good antimalarial activity.[5] Moreover, Suckling and Khalaf have shown in several studies that DNA minor groove binders related to distamycin are good and efficient antibacterial agents.[6] In particular, they have shown that peptide derivatives (amide isosters) show good DNA binding affinity and antibiotic activity.

It is generally accepted that DNA minor groove binders, which interact with DNA by means of hydrogen bonds (HBs) and van der Waals and ionic forces, should have a curved structure to optimally fit into the groove. In fact, studies on many synthetic derivatives such as furamidine and furimidazole have shown that the curvature degree plays an important role in the binding.[7] Thus, on the one hand, it was observed that furamidine exhibits a too open molecular curvature that prevents the furan ring from optimizing its contacts with the groove floor.[8] On the other hand, Boykin et al. reported a thiophenebenzimidazole analogue of furamidine whose binding strength was increased as a result of a decreased curvature, thereby allowing the central moiety of the molecule to establish optimized contacts with the minor groove.[9] Moreover, it was found that linear derivatives, which differ from the classical minor groove binder criteria, rendered very good binding affinity by hydrogen-bonding to water molecules. It seems that these linear compounds form HBs with water molecules to link to the DNA base pairs at the floor of the minor groove, forming the corresponding DNA complex; hence, these water molecules provide the curvature required.[10,11] In addition, Wilson et al. have reported a compound that deviates from the curvature theory by forming a "seesaw" complex with the minor groove.[12] Additionally, different oligoamides have been prepared that are capable of highly specific DNA binding;[13] further research has also resulted in the preparation of hairpins polyamides that fit snuggly into the groove.[14] The degree of polyamide curvature is a relevant issue when studying the facility of such compounds

Received: March 1, 2012
Published: April 12, 2012

dx.doi.org/10.1021/jm300296f | J. Med. Chem. 2012, 55, 4397−4406

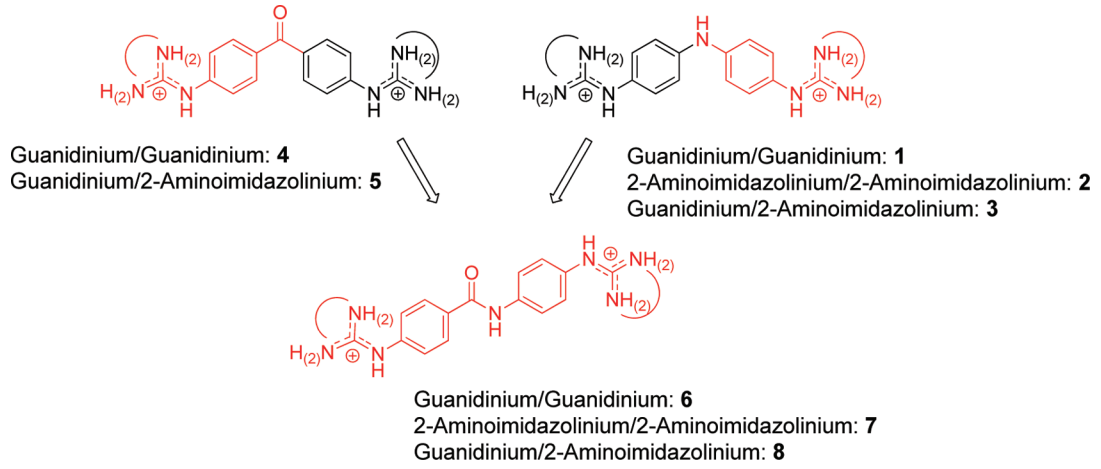

Figure 1. Design of peptide-linked dicationic derivatives **6**, **7**, and **8**.

to bind into the DNA minor groove, and it has been recently studied.[15]

As mentioned, we have previously reported a number of symmetric and asymmetric bis-guanidinium or -2-aminoimidazolinium diaromatic compounds that strongly bind to DNA with significant AT sequence selectivity.[1] Moreover, their interactions with DNA were investigated by various biophysical techniques such as thermal denaturation, circular dichroism (CD), surface plasmon resonance (SPR), and isothermal titration calorimetry (ITC), and their mode of binding was confirmed by linear dichroism (LC) as being minor groove binders.[2] In particular, those molecules with a NH or a CO linker (Figure 1) gave very interesting results, the NH-linked ones displaying the largest binding affinity in each series (symmetric bis-guanidinium (**1**) and bis-2-aminoimidazolinium (**2**) and asymmetric guanidinium/2-aminoimidazolinium (**3**)) with good AT selectivity, whereas from the two CO-linked analogues **4** and **5**, the asymmetric guanidinium/2-aminoimidazolinium (**5**) displayed unusual CG binding.

Taking into account these compounds and considering that many known minor groove binders (i.e., netropsin or distamycin) contain peptide bonds (-CONH-) that allow hydrogen bonding to DNA bases, we present here the preparation and DNA affinity evaluation of a series of symmetric and asymmetric peptide linked derivatives carrying guanidinium-like cations (compounds **6**, **7**, and **8**; see Figure 1). The reasoning behind this design is that the combination of a HB acceptor such as CO with a HB donor such as NH could provide extra points of contact, resulting in an increased binding affinity for DNA.

The proposed peptide-linked dicationic molecules **6**, **7**, and **8** would be linear structures, but as we have discussed before, in principle this should not be a problem for their binding into the DNA minor groove. Additionally, the mono-guanidinium (**9**) and mono-2-aminoimidazolinium (**10**) peptide derivatives have also been prepared. Finally, to investigate the binding of all these compounds to DNA, different biophysical techniques have been used such as thermal denaturation and CD to measure their binding strength, SPR to obtain information on their selectivity, and ITC to find the relevant thermodynamic quantities and binding constants.

RESULTS

Computational Study. By use of the crystal structure of a peptide-linked bis-isouronium analogue[16] as a template, a model for the bis-guanidinium derivative (**6**) was prepared and optimized using DFT methods (B3LYP/6-31+G*, mimicking water solvation with PCM). Two models were calculated, one with the isolated peptide-linked molecule and the other using hydrogen bonded water molecules to elongate the curvature of the dicationic structure (Figure 2). In the case of the isolated

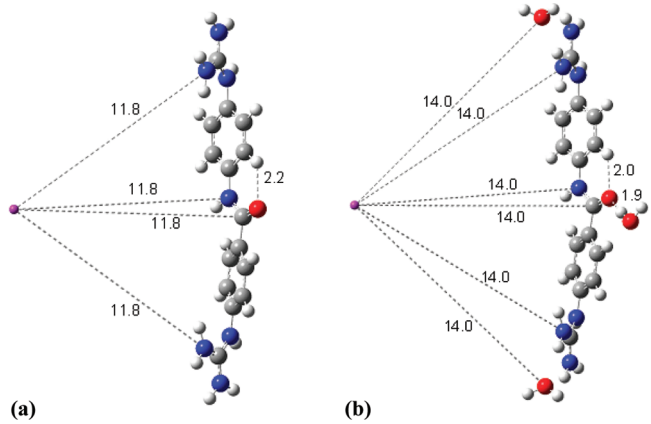

Figure 2. DFT (B3LYP/6-31+G*, PCM-water) optimized structures of (a) bis-guanidinium peptide linked derivative showing a curvature radius of 11.8 Å and (b) the same compound complexed with three water molecules showing a radius of 14 Å. In both cases an intramolecular interaction between the peptide C═O group and one of the aromatic H atoms was found. Graphics and radius determination were done with Gaussview 5.0 (C atoms are represented in gray, N atoms in blue, O atoms in red, and H atoms in white).

dication (Figure 2a), using as reference a NH_2 of each of the guanidinium groups and the N and C atoms of the peptide linker, a curvature of a 11.8 Å radius was obtained.

In the model containing the water molecules, two of them were used to complex each of the guanidinium cations while a third water molecule was hydrogen bonded to the peptide C═O group in order to avoid a double "intramolecular" HB with one of the end side water molecules, thus avoiding the bending of the molecule. In this case, the same points were used as reference to calculate the curvature radius plus the O atoms of each of the water molecules at both ends of the system, and a value of 14 Å was obtained (see Figure 2b). The water molecules on both ends of the molecule have extended

dx.doi.org/10.1021/jm300296f | J. Med. Chem. 2012, 55, 4397−4406

Scheme 1. Synthesis of Asymmetric Mono- and Bis-guanidinium-like Hydrochloride Salts 8, 9, and 10[a]

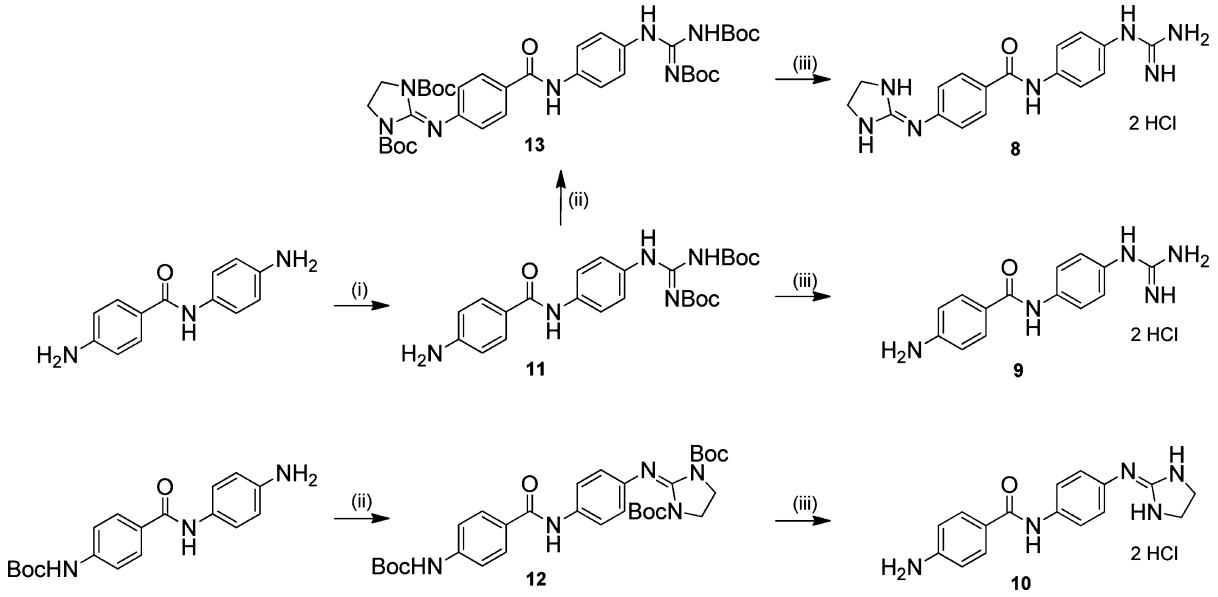

[a]Reagents and conditions: (i) *N*,*N*′-bis(*tert*-butoxycarbonyl)thiourea, $HgCl_2$, NEt_3, DMF, room temp; (ii) *N*,*N*′-bis(*tert*-butoxycarbonyl)imidazoline-2-thione, $HgCl_2$, NEt_3, DMF, room temp; (iii) TFA, DCM, room temp followed by Amberlyte resin, H_2O, room temp.

the arc, and for that reason the radius is larger. However, this is still a reasonable curvature radius to fit into the minor groove.

From this simple computational model it was evident that these peptide-linked dications (as isolated structures as much as networked with water molecules) will adopt a reasonable curvature to fit into the DNA minor groove.

Chemistry. On the basis of our previous experience and taking into account the encouraging synthetic results obtained in our group,[17,18] the guanidylation and 2-aminoimidazolylation processes to achieve the present target molecules were performed following our established methodology. This consists of the reaction of the peptide-linked (mono)deactivated aromatic diamine or the mono-Boc-protected derivative (both commercially available) with *N*,*N*′-bis(*tert*-butoxycarbonyl)thiourea (guanidine precursor) or *N*,*N*′-bis(*tert*-butoxycarbonyl)-imidazoline-2-thione[14] (2-aminoimidazoline precursor) assisted by mercury(II) chloride and in the presence of an excess of triethylamine in DMF (Scheme 1). Deprotection of the Boc intermediates thus obtained with trifluoroacetic acid/dichloromethane and further treatment with Amberlyte resin in water lead to the hydrochloride salts of the target molecules (Scheme 1).[14,15] In the preparation of the Boc-protected mono-guanidinium-like compound **11**, reaction occurs preferentially at the amino group in para position with respect to the peptide NH group which is more activated. The synthesis of **9** and **10** was previously reported by us using different strategies.[3]

In the case of the asymmetric derivative, the preparation of the Boc-protected compound **13** required a careful strategy. Considering the nature of the peptide linker, those derivatives with the guanidinium or the 2-aminoimidazolinium moiety in position para to the aromatic NH group are preferentially formed. Thus, it could be possible to first guanidylate the diamine and then 2-aminoimidazolydate it or the other way around, first introducing the 2-aminoimidazoline ring and then the guanidinium precursor. However, in our experience, early introduction of the 2-aminoimidazoline moiety usually results in very poor yields due to decomposition during chromatographic purification in silica support. For that reason, Boc-guanidylation of the aromatic diamine was first performed yielding only compound **11**, which was subsequently reacted with the 2-aminoimidazolinium precursor producing the asymmetric Boc-protected derivative **13** (Scheme 1). The Boc-protected guanidine derivative substituted in position para to the aromatic CO group was never obtained because of the deactivating effect of such a carbonyl group.

Total yields obtained in the preparation of the two mono-guanidinium-like derivatives were 55% (compound **9**) and 60% (compound **10**), and for the asymmetric guanidinium/2-aminoimidazolinium **8** a 35% yield was achieved. Boc deprotection reactions worked with very good yields around 92−95%.

Thermal Denaturation Assays: Relative Binding Affinity. The interaction of compounds **3** and **5**−**10** with unspecific salmon sperm DNA was evaluated by means of thermal denaturation experiments, enabling a quick qualitative evaluation for the relative DNA binding affinities as we have previously shown.[1,3] In addition, AT specific interactions were investigated by performing these thermal denaturation experiments with poly(dA·dT)$_2$ in compounds **6**−**8**. The melting temperature obtained for all these molecules with unspecific salmon sperm DNA and the AT homopolymer poly(dA·dT)$_2$ is presented in Table 1 together with previous results reported by us for NH-linked and CO-linked derivatives and with the AT specific poly(dA)·poly(dT) oligonucleotide, for the sake of comparison.

The results presented in Table 1 show that all molecules displayed a stabilizing effect on natural DNA where compounds **9** and **10** show minimal affinity for mixed sequence DNA. Furthermore, compound **10** reveals an extra stabilizing effect on natural DNA due to the hydrophobic nature of the 2-aminoimidazoline cation. These results were somewhat surprising given the fact that the aromatic rings are virtually planar thus allowing for optimized contacts within the groove.

When the second amino group was functionalized by another cationic group, the affinity rose significantly with a 5- to 10-fold

dx.doi.org/10.1021/jm300296f | J. Med. Chem. 2012, 55, 4397−4406

Table 1. Summary of Thermal Denaturation Results Obtained for All Peptide-Linked Structures Prepared by Rozas and Co-Workers in the Present and Previous Studies[d]

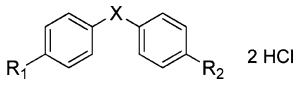

Compd.	X	R_1	R_2	$\Delta T_{m(SS)}$ Salmon sperm DNA[a]	$\Delta T_{m(AT)}$ poly(dA•dT)$_2$ DNA[b]	$\Delta T_{m(AATT)}$ poly(dA)•poly(dT) DNA[c]
1[3]	NH			-	-	29.6[3]
2[3]	NH			-	-	38.5[3]
3[1]	NH			12[1]	17.5[1]	35.1[1]
4[3]	CO			-	-	27.6[3]
5[1]	CO			8[1]	15[1]	32[1]
6[3]	CONH			11	20	40.1[3]
7[3]	CONH			12.5	29	47.1[3]
8	CONH			10	26.1	-
9	CONH	NH_2		1	-	-
10	CONH	NH_2		2	-	-

[a]DNA melting temperature in phosphate buffer (10 mM) is 69 °C. [b]P/D = 10. Poly(dA·dT)$_2$ T_m in phosphate buffer (10 mM) is 47 °C (as in ref 1). [c]P/D = 3. Poly(dA)·poly(dT) T_m in MES buffer (10 mM) is 43 °C (as in ref 3). [d]The increment in DNA thermal melting (ΔT_m, °C) is presented in unspecific salmon sperm DNA as well as in specific AT oligonucleotides such as poly(dA·dT)$_2$ and poly(dA)·poly(dT).

Scheme 2. Structures of the Hairpins Used for the SPR Studies

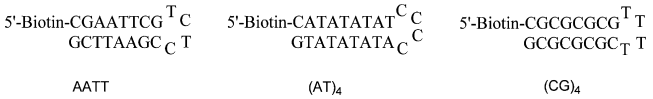

difference (with a $\Delta T_{m(SS)}$ between 10 and 12.5). This is justified because of both (i) the addition of an extra point of contact in terms of a HB donor on the guanidine or 2-aminoimidazoline functionality and (ii) the additional ionic interaction between the dicationic molecule and the negatively charged DNA. Furthermore, the order of binding affinity found is **7** > **8** > **6**, and this seems to indicate that the hydrophobic nature of the 2-aminoimidazoline functionality plays a role in increasing the binding affinity.

Considering these promising results, the experiments were repeated by replacing the mixed sequence DNA for the AT homopolymer as a method to investigate sequence selectivity. The minor groove of the AT polymer is narrower compared to natural DNA, allowing for a tighter fit and for the formation of closer contacts with the walls of the minor groove. The results from Table 1 show the preferred binding to AT sequences with up to 2.6-fold difference. Moreover, when the guanidine functionality was replaced by a 2-aminoimidazoline group, the affinity for AT sequences rose dramatically from a 1.8- to a 2.6-fold difference. This can be attributed to the presence of an extra ethylene bridge which has the ability to form van der Waals contacts with the walls of the minor groove. From the results presented, the presence of the extra bridge is necessary for increasing the sequence selectivity of these particular compounds.

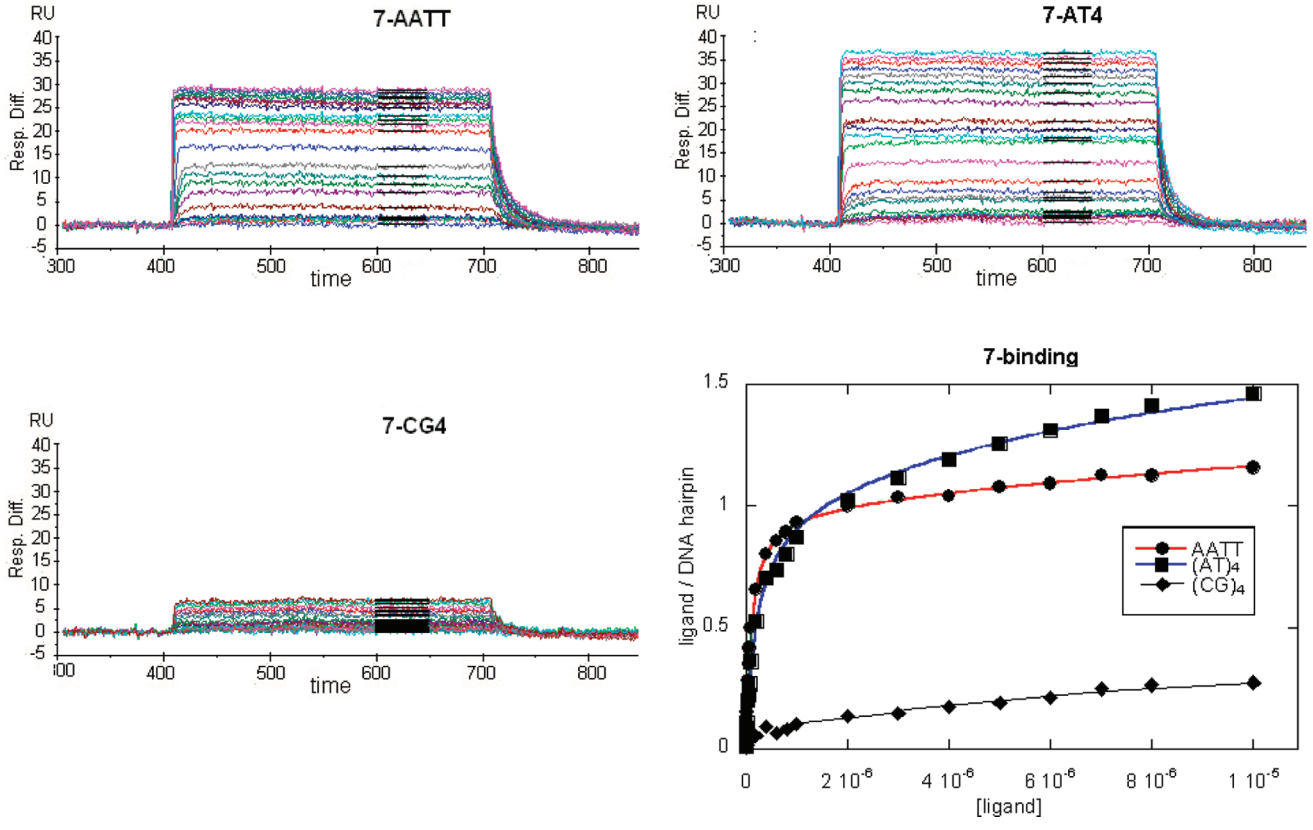

Figure 3. Sensorgrams for the interaction of compound **7** with the AATT hairpin (upper left), with (AT)$_4$ hairpin (upper right), with (CG)$_4$ hairpin (bottom right) and in the bottom left the fits of **7** with AATT (squares), with (AT)$_4$ (circles), and with (CG)$_4$ (diamonds).

dx.doi.org/10.1021/jm300296f | J. Med. Chem. 2012, 55, 4397−4406

Table 2. Binding Constants (M^{-1}) Obtained from SPR Experiments for Compounds 6 and 7 with AATT, $(AT)_4$, and $(CG)_4$ Hairpins[a]

	K ($\times 10^5$ M^{-1})			
compd	AATT	$(AT)_4$	$(GC)_4$	sequence specificity
	71.0	18.0	<1[b]	AT
7	93.7	47.7	<1[b]	AT
3	6.4[c]		<1[b]	AT
5	2.7[c]		3.6[c]	AT
proflavine	5.7	12.2	6.5	none

[a]The corresponding binding constants for asymmetric dications NH-linked **3** and CO-linked **5** and for a classical intercalator proflavine are shown for comparison. [b]There is not enough signal-to-noise ratio to get a binding constant for $(GC)_4$. [c]Reference 2.

Surface Plasmon Resonance (SPR). SPR is a quantitative method to evaluate the binding of small molecules to specific oligonucleotides and provides accurate binding constants. In the present study, the hairpins shown in Scheme 2 (AATT, AT, and CG) have been used to determine the binding of some of the peptide-linked dications.

Sensorgrams for compound **7** showing strong binding [to AATT and $(AT)_4$] and weak binding [to $(CG)_4$] are presented in Figure 3. All the sensorgrams recorded for the binding to AT hairpins (for compounds **6** and **7** and also those previously reported by us in ref 2 for compounds **3** and **5**) show rapid kinetics of association and dissociation from low to high concentrations, indicating that these compounds can enter and leave the minor groove with a relatively low energetic barrier. However, the sensorgrams obtained for compounds **6** and **7** binding to CG hairpins (see the corresponding for compound **7** in Figure 3, bottom left) show very small increments, indicating reduced binding.

The binding constants (K) for compounds **6** and **7** to the three DNA hairpin duplexes shown in Scheme 2 were determined by plotting the steady-state response values versus the concentration of the free compounds and fitting as described in the Experimental Section. The results obtained are presented in Table 2. SPR errors in K for AATT and $(AT)_4$ are ±20% based on repeat experiments for compounds **6** and **7**. For the lower binding constants for **3**, **5**, and proflavine, the errors increase to ±30% for all DNAs tested.

In general, larger binding constants are obtained for the interactions with AATT and $(AT)_4$ than with $(CG)_4$ and only a single strong AT binding site is observed for these compounds. This clearly indicates a strong AT sequence specificity for the binding of these peptide-linked dications which probably are pure minor groove binding agents. Moreover, from a comparison of the binding constants of compounds **6** and **7** with those of the intercalator proflavine (see Table 2), the high selectivity toward AT sequences is more evident confirming even further the pure minor groove binder character of these compounds.

Circular Dichroism Studies. Given the demonstrated affinity of these molecules to poly(dA·dT)$_2$ sequences as indicated by the thermal denaturation results, circular dichroism (CD) experiments were carried out. These have proved useful for determining binding mode and can provide information on conformational changes in the polynucleotides as well as offer a means to evaluate the binding stoichiometry.[19] A CD spectrum monitors the induced chiral environment of a molecule on binding to DNA. Thus, it can be used as a

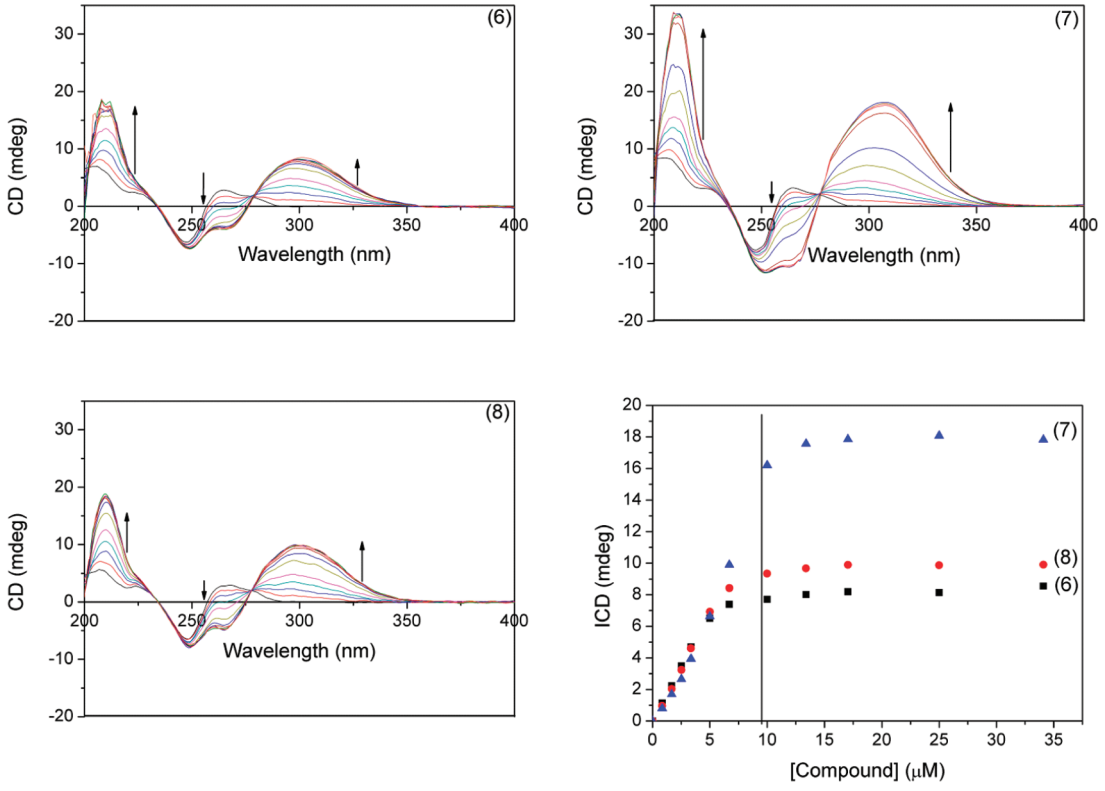

Figure 4. CD titration spectra of poly(dA·dT)$_2$ [37.5 μM in base] on addition of the peptide linked compounds **6** (upper, left), **7** (upper, right), and **8** (bottom, left) with a Bp/D ratio from 22.4 to 0.56. Also shown are CD saturation curves for **6**, **7**, and **8** (bottom, right); the dark line indicates where saturation occurs. Experiments were run in phosphate buffer (pH 7) at T = 25 °C.

dx.doi.org/10.1021/jm300296f | J. Med. Chem. 2012, 55, 4397−4406

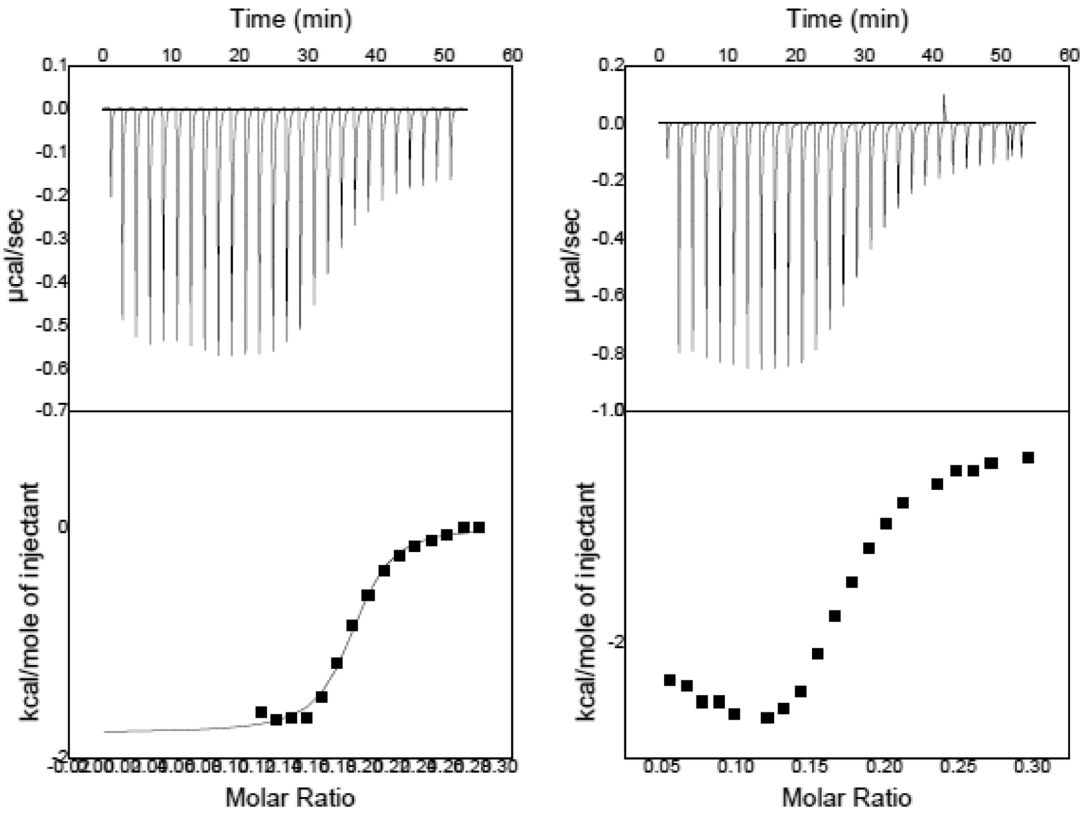

Figure 5. ITC results obtained for the bis-2-aminoimidazoline compound **7** (left) and for the guanidine/2-aminoimidazoline derivative **8** (right) in poly(dA·dT)$_2$. These plots show corrected experimental data, and the experiments were done in phosphate buffer at 25 °C.

diagnostic for the mode of binding where compounds that bind to the minor groove are in proximity to the chiral sugar, resulting in a large induced CD signal (ICD).[20] In particular, minor groove binders, because of their proximity to chiral sugar molecules, typically exhibit strong ICD signals, whereas intercalators show little or no ICD signals.

CD titration experiments were carried out to evaluate the binding mode and the subsequent binding stoichiometry for compounds **6**, **7**, and **8** to random sequenced DNA and poly(dA·dT)$_2$ homopolymer (Figure 4). The free compounds have no CD signal by itself; however, in the presence of DNA a large ICD signal is formed at 302, 308, and 303 nm for **6**, **7**, and **8**, respectively. The magnitude of these ICD signals is related to the chiral environment as previously mentioned, and thus, molecules interacting in the minor groove will induce a larger signal change.[21]

Titrations with natural DNA (spectra in Supporting Information) result in the formation of an ICD signal at 280 nm accompanied by small changes in the DNA spectrum on addition of the compounds. In contrast, when the experiments were repeated in the presence of the poly(dA·dT)$_2$ homopolymer, large ICD signals were observed in the region from 300 to 310 nm, suggesting that the compounds interact strongly with the minor groove. Moreover, small changes in the DNA signal at 260 nm were observed when the experiments were carried out with natural DNA whereas large ICD signals were observed in the AT homopolymer CD spectra, implying that significant changes in the minor groove of the AT homopolymer occurred on addition of the compound. As the minor groove for AT sequences is much narrower than that of natural DNA with a 32% GC content, the binding of these molecules might cause more significant changes in the structure and hence in the DNA spectrum. Moreover, it could be postulated that the binding of these molecules causes significant widening of the groove, as evidenced from the mentioned changes in the DNA spectrum. However, interpretation of this region is difficult to make because the compound absorption occurs nearby.

Moreover, the ICD signal for the asymmetric guanidine/2-aminoimidazoline compound **3** (NH linker) was considerably larger than that of its analogue **8** (peptide linker), although the DNA binding of the latter was more favorable than the former.[2] The larger induced CD signal may suggest that the diphenyl torsional angle is larger when the amide linker is replaced by the -NH- group.[8]

The binding stoichiometry was evaluated using saturation plots (Figure 4, bottom right), and it supports a Bp/*D* binding ratio of 4, which is a good agreement with our previous compounds.

Isothermal Titration Calorimetry. Calorimetric titrations allow for the evaluation of the binding enthalpy and equilibrium association constant in one experiment.[22] In Figure 5 the titration results representing exothermic reactions for all binding experiments for compounds **7** and **8** are shown.

Furthermore, the equilibrium association constant (K; $\Delta G = nRT \ln K$) thus obtained and the binding enthalpy (H) allow the calculation of the binding entropy (S) from the relationship $\Delta G = \Delta H - T\Delta S$. A summary of the thermodynamic parameters is presented in Table 3. The binding thermodynamics reveal favorable enthalpic and entropic contributions where the enthalpy varies by 1 kcal mol^{-1}, while the entropic contribution varies from 13.9 to 20.1 cal mol^{-1} K^{-1}.

dx.doi.org/10.1021/jm300296f | J. Med. Chem. 2012, 55, 4397−4406

Table 3. Thermodynamic Parameters, Binding Stoichiometry, and Binding Constants Calculated for Compounds 7 and 8 by ITC with Poly(dA·dT)$_2$ (Phosphate Buffer)

compd	binding stoichiometry	K ($\times 10^5$ M^{-1})	ΔH^0 (kcal mol^{-1})	ΔS^0 (cal mol^{-1} K^{-1})
7	0.187 ± 0.001	4.9 ± 0.8	−1.78 ± 0.04	20.1
8	0.193 ± 0.005	1.54 ± 0.63	−2.55 ± 0.09	15.9

Remarkably, the binding enthalpy contribution for these compounds becomes more negative following the order of **8** < **7**, suggesting that replacing the guanidine functionality for the 2-aminoimidazoline group results in the formation of more favorable interactions. Considering that these molecules exhibit distinct structural similarities and accounting for the main difference being the ethylene bridge on the 2-aminoimidazoline functionality, the resulting decrease in enthalpy could be attributed to the extra van der Waals contacts from these cyclic functionalities.

DISCUSSION AND CONCLUSIONS

In the present study, we have focused on a series of amide linked molecules that have demonstrated the strongest binding affinity in our current series of guanidine and 2-aminoimidazoline molecules. Thus, this study served to address the following questions: (i) What, if any, is the relevance for the radius of curvature in binding, and (ii) what is the importance of a functionalized linker with a HB donor and acceptor?

Many detailed studies have focused on the design of molecules that complement the concave structure of the DNA minor groove. Nevertheless, some linear molecules have attracted attention because of their unpredictable higher affinity for the DNA minor groove where a water molecule allows the completion of the required curvature. This allowed us to realize the importance of water molecules that serve as HB bridges, thus allowing the formation of an appropriate radius of curvature of subsequent molecules. These interactions have found new scope for investigations for targeting the minor groove.

As a result of calculations performed on bis-guanidinium derivatives **1** (NH) and **4** (CO), we have observed that the curvature radius of these compounds (8.7 and 8.2 Å, respectively; see Supporting Information) strongly differs from that obtained for compound **6** (11.8 Å), which could explain the differences in binding. Furthermore, berenil, which has a radius of curvature of 14 Å, demonstrates significant affinity for the minor groove of AT sequences. Given that the radius of **8** is 11.8 or 14 Å when water molecules are incorporated (as calculated computationally with B3LYP/6-31+G* and PCM-water), their potential as minor groove targeting drugs is evident. Dickerson and co-workers have done a detailed quantitative analysis of the appropriate curvature and position of functional groups for optimum binding to the DNA minor groove.[23] On the basis of the helical curvature of B-form DNA and known minor groove binders, they conclude that a 20−25 Å radius of curvature is optimal for minor groove binding. However, there is some flexibility in this range due to some possible induced fit conformational changes in both the binding compound and DNA.

The nature of the strong interaction with AT sequences can also be explained by the fact that the CO group from the amide linker can form a weak HB interaction with the ortho-H with respect to the linker (bond distance of 2.0 Å), thus making the amide linker and the resulting aromatic moiety coplanar allowing for a better fit into the narrow groove of AT sequences. Moreover, we have observed that in the crystal structure of a related compound with an O linker,[24] the angle between the phenyl rings is 72°, and in the computed bis-guanidinium NH and CO derivatives this angle was found to be 161° and 157°, respectively; i.e., they are almost perpendicular to each other. This indicates that compounds **1** and **4** need to undergo a torsion to fit within the minor groove, and we have previously evaluated the energy required for this type of torsion to be around 6 kcal mol^{-1} (for asymmetric guanidine/2-aminoimidazoline derivatives with NH or CO as linkers[2]). On the contrary, the phenyl rings on the peptide-linked derivatives are coplanar, and hence, such torsion would not be required prior to binding into the minor groove and this binding would be energetically more favored.

The dicationic structures with a linear Ph-CO-NH-Ph core presented in this study show a favored curvature by means of the guanidinium cations and exhibit a better length and fitting than the previously prepared bis-guanidine-like minor groove binders with only a NH or a CO linker. The crystal structure of the NH-linked bis-2-aminoimidazoline diaromatic molecule complexed to an AT oligonucleotide[25] shows that this linker clearly points outside the groove. In a similar manner, the linkers from compounds **1** and **4** (NH and CO, respectively) are expected to point out of the groove; however, the NH of the amide linker is pointing inside the groove (see Figure 2), thus increasing the probability of extra HBs forming with the inner side of the groove improving the binding.

By use of our already established methodology, three new peptide-linked compounds have been prepared: an asymmetric guanidinium/2-aminoimidazolinium diaromatic derivative and the mono-guanidinium and mono-2-aminoimidazolinium derivatives compounds **8**, **9**, and **10**, respectively.

Thermal melting denaturation experiments were carried out for these compounds and compared with previous results obtained for related peptide-linked and CO- or NH-linked diaromatic bis-guanidinium-like derivatives. Mono-guanidinium-like compounds showed poor binding; however, the bis-guanidinium-like peptide-linked derivatives showed very strong binding to DNA with selectivity for the AT sequences, indicating minor groove preference. Compound **7** shows the highest affinity toward AT sequences with a ΔT_m value 1.1 and 1.3 times that of **8** and **6**, respectively, illustrating that the 2-aminoimidazoline ring promotes a higher affinity for AT sequences. Given that the only difference between both cations is the extra ethylene bridge, these results can indicate that the extra van der Waals contact with the minor groove increases both the selectivity and affinity of these molecules significantly.

Finally, other biophysical experiments on the peptide-linked compounds **6**, **7**, and **8** were carried out using SPR, CD, and ITC techniques, all of them indicating strong binding to DNA in particular to the minor groove. The binding constants obtained with SPR for compounds **6** and **7** and for the guanidine/2-aminoimidazoline dications with a NH or a CO linker (**3** and **5**) clearly show that the peptide-linked derivatives bind more strongly despite the presumed linearity of their core. Despite the fact that the SPR and ΔT_m values were obtained at

dx.doi.org/10.1021/jm300296f | J. Med. Chem. 2012, 55, 4397−4406

different salt concentrations (92 and 0 mM NaCl, respectively), qualitative comparison of these binding constants with the ΔT_m values using poly(dA·dT)$_2$ and poly(dA)·poly(dT) (see Table 1) shows similar trends, the best agreement found between ΔT_m and the AATT binding constants indicating a possible preference for the minor groove.

Recently, Terame and co-workers[26] have reported the interactions of a guanidine derivative (amiloride) and DNA, suggesting that there may be a possible repulsion between the methyl group in the thymine base and the cationic guanidinium group in the major groove and that this may lead the molecule to bind in the minor groove where no such repulsion is possible. A similar reason could be behind the minor groove binding of our molecules. Moreover, they also hint that the interaction of the guanidinium cation and the phosphate backbone could be possible in the minor groove, favoring these compounds to lay into the DNA minor groove.

In the ITC experiments, each of the compounds displayed larger binding constants than previous molecules in this series.[2] Comparison of the binding constants indicated that the order of binding strength **7** > **8** correlates with the thermal denaturation results. The large entropy observed for **7** seems to be responsible for the increased binding constant. However, the order of the enthalpies is reversed, which could indicate that the guanidine functionality (present in compound **8**) forms stronger hydrogen bonds than the 2-aminoimidazoline one. This is in agreement with the hypothesis that the bis-2-aminoimidazoline **7** has more freedom inside the narrow minor groove than **8**. However, further investigation is required to confirm this.

In summary, the presence of a planar amide linker between the phenyl rings seems to provide the bis-cataionic ligands with the orientation ideal to better fit into the minor groove and to establish very favorable interactions.

EXPERIMENTAL SECTION

Computational Methods. The systems have been optimized using the Gaussian 09[27] package at the B3LYP[28] computational level with the 6-31+G*[29] basis sets. Frequency calculations have been performed at the same computational level to confirm that the resulting optimized structures are energetic minima. Effects of water solvation have been included by means of the SCRF-PCM approaches implemented in the Gaussian 09 package including dispersion, repulsion, and cavitation energy terms of the solvent in the optimization. The electron density of the complexes has been analyzed within the atoms in molecules (AIM) theory[30] to confirm the formation of hydrogen bonds.

Compounds, DNA, and Buffers. The syntheses of compounds **1**, **2**, **3**, **4**, and **5** have been previously described by us.[3] The identity of all compounds was determined by ^{1}H and ^{13}C NMR, IR, and HRMS and their purity assessed by elemental analysis. Natural salmon sperm DNA and poly(dA·dT)$_2$ were purchased and used as received. The concentration of the DNA solutions was determined spectrophotometrically using an extinction coefficient of 6600 cm^{-1} M^{-1}. Phosphate buffer contained 10 mM Na_2HPO_4/NaH_2PO_4 adjusted to pH 7 and was prepared using Millipore water.

Chemistry. All the commercial chemicals were obtained from usual suppliers and were used without further purification. Dry solvents were prepared using standard procedures, according to Vogel, with distillation prior to use. Chromatographic columns were run using silica gel 60 (230−400 mesh ASTM) or aluminum oxide (activated, Neutral Brockman I STD grade 150 mesh). Solvents for synthetic purposes were used at GPR grade. Analytical TLC was performed using silica gel plates or aluminum oxide plates. Visualization was by UV light (254 nm). NMR spectra were recorded in a spectrometer operating at 400.13 and 600.1 MHz for ^{1}H NMR and at 100.6 and 150.9 MHz for ^{13}C NMR. Shifts are referenced to the internal solvent signals. HRMS spectra were measured using methanol as the carrier solvent. Melting points are uncorrected. Infrared spectra were recorded on a spectrometer equipped with Universal ATR sampling accessory. Elemental analyses (C, H, N) of the target compounds, which were performed at the Microanalysis Laboratory (School of Chemistry and Chemical Biology, University College Dublin, Ireland), are within ±0.4% of the calculated values, confirming ≥95% purity. Fractional moles of water frequently found in amidinium-like salts could not be prevented despite 24−48 h of drying in vacuum.

General Procedure for the Boc-Guanidylation or Boc-2-Aminoimidazolylation of Aromatic Amines: Method 1. Each of the corresponding amines was treated in DMF at 0 °C with 1.1 equiv of mercury(II) chloride, 1.0 equiv of *N*,*N*′-di(*tert*-butoxycarbonyl)-imidazolidine-2-thione (for the 2-aminoimidazoline precursors) or *N*,*N*′-di(*tert*-butoxycarbonyl)thiourea (for the guanidine precursors), and 3.1 equiv of NEt_3. The resulting mixture was stirred at 0 °C for 1 h and for the appropriate duration at room temperature. Then the reaction mixture was diluted with EtOAc and filtered through a pad of Celite to get rid of the mercury sulfide formed. The filter cake was rinsed with EtOAc. The organic phase was washed with water (2 × 30 mL), washed with brine (1 × 30 mL), dried over anhydrous Na_2SO_4, and concentrated under vacuum to give a residue that was purified by silica gel (guanidine precursors) or neutral alumina column flash chromatography (2-aminoimidazoline precursors), eluting with the appropriate hexane/EtOAc mixture.

4-Amino-*N*-[4-*N*′,*N*″-di(*tert*-butoxycarbonyl)guanidinophenyl]-benzamide (11). Following method 1 and with purification by flash chromatography in silica (hexane/ethyl acetate, 2:1), a white solid was obtained (58%): mp 136−138 °C; ^{1}H NMR ($CDCl_3$) δ 1.40 (s, 9H, $(CH_3)_3$), 1.52 (s, 9H, $(CH_3)_3$), 5.77 (brs, 2H, NH_2), 6.61 (d, 2H, J = 8.4 Hz, Ar.), 7.46 (d, 2H, J = 8.4 Hz, Ar.), 7.69−7.72 (m, 4H, Ar.), 9.82 (brs, 1H, NH), 9.95 (brs, 1H, NH), 11.47 (brs, 1H, NH); ^{13}C NMR ($CDCl_3$) δ 27.6, 27.9 ($(CH_3)_3$), 78.7, 83.3 ($\underline{C}(CH_3)_3$), 112.5, 120.0, 120.9, 123.1, 123.2, 129.3, 136.8, 144.4 (Ar.), 152.1, 153.0 (CO), 162.7 (CN), 165.1 (CO). ν_{max} (film)/cm^{-1}: 3474, 3373, 2984 (NH), 1718, 1647, 1624, 1608 (CO, CN).

4-(*N*-*tert*-Butoxycarbonylamino)-*N*-{4-[*N*′,*N*″-di(*tert*-butoxycarbonyl)-2-aminoimidazolino]phenyl}benzamide (12). Following method 1 and with purification by flash chromatography in alumina (hexane/ethyl acetate, 2:5), a white solid was obtained (65%): mp 216−218 °C; ^{1}H NMR (DMSO-d_6) δ 1.30 (s, 18H, $2(CH_3)_3$), 1.51 (s, 9H, $(CH_3)_3$), 3.77 (s, 4H, CH_2 Im), 6.83 (d, 2H, J = 8.5 Hz, Ar.), 7.59 (d, 2H, J = 8.5 Hz, Ar.), 7.63 (d, 2H, J = 8.5 Hz, Ar.), 7.91 (d, 2H, J = 8.5 Hz, Ar.), 9.70 (brs, 1H, NH), 9.96 (brs, 1H, NH), 10.14 (brs, 1H, NH); ^{13}C NMR (DMSO-d_6) δ 28.8, $(2(CH_3)_3)$, 29.4 ($(CH_3)_3$), 44.2 (CH_2 Im), 80.8 ($\underline{C}(CH_3)$), 82.7 ($\underline{C}(CH_3)$), 118.4, 122.0, 122.1, 129.4, 129.8, 135.1, 140.2, 143.8, (Ar.), 145.6, 151.0, (CO), 153.9 (CN), 165.7 (CO). ν_{max} (film)/cm^{-1}: 3364, 3276 (NH), 1731, 1710, 1655, 1594 (CO, CN).

4-[*N*′,*N*″-Di(*tert*-butoxycarbonyl)-2-aminoimidazolino]-*N*-[4-*N*′,*N*″-di(*tert*-butoxycarbonyl)guanidinophenyl]benzamide (13). Following method 1 from **11** and with purification by flash chromatography in alumina (hexane/ethyl acetate, 1:1), a white solid was obtained (65%): mp 112−114 °C; ^{1}H NMR (DMSO-d_6) δ 1.28 (s, 18H, $(CH_3)_3$ Im), 1.47 (s, 9H, $(CH_3)_3$), 1.52 (s, 9H, $(CH_3)_3$), 3.79 (s, 4H, CH_2 Im), 6.93 (d, 2H, J = 8.5 Hz, Ar.), 7.49 (d, 2H, J = 9.0 Hz, Ar.), 7.76 (d, 2H, J = 9.0 Hz, Ar.), 7.88 (d, 2H, J = 8.5 Hz, Ar.), 9.97 (brs, 1H, NH), 10.08 (brs, 1H, NH), 11.47 (brs, 1H, NH); ^{13}C NMR (DMSO-d_6) δ 27.5 ($(CH_3)_3$ Im), 27.7, 27.9 ($(CH_3)_3$ Gu), 43.0 (CH_2), 81.7 ($\underline{C}(CH_3)_3$ Gu), 82.4 ($\underline{C}(CH_3)_3$ Gu), 83.1 ($\underline{C}(CH_3)_3$ Im), 119.5, 120.4, 123.3, 127.4, 128.4, 131.9, 136.5, 140.2 (Ar.), 152.1, 152.2, 153.0, 162.8, 164.9, 170.4 (CO, CN). ν_{max} (film)/cm^{-1}: 3386, 3252, 3155 (NH), 1764, 1731, 1717, 1668, 1645, 1634 (CO, CN).

General Procedure for the Synthesis of the Hydrochloride Salts: Method 2. Each of the corresponding Boc-protected precursors (0.5 mmol) was treated with 15 mL of a 50% solution of trifluoroacetic acid in DCM for 3 h. After that time, the solvent was eliminated under vacuum to generate the trifluoroacetate salt. This salt was dissolved in 20 mL of water and treated for 24 h with IRA400

Amberlyte resin in its Cl^- form. Then the resin was removed by filtration and the aqueous solution washed with DCM (2 × 10 mL). Evaporation of the water afforded the pure hydrochloride salt. Absence of the trifluoroacetate salt was checked by ^{19}F NMR.

Dihydrochloride Salt of 4-(2-Aminoimidazolino)-*N*-(4-guanidinophenyl)benzamide (8). Following method 2 starting from compound **13**, a white solid was obtained (94%): mp 220 °C (dec); ^1H NMR (D_2O) δ 3.66 (s, 4H, CH_2), 7.24 (d, 2H, J = 7.0 Hz, Ar.), 7.41 (d, 2H, J = 8.5 Hz, Ar.), 7.51 (d, 2H, J = 8.5 Hz, Ar.), 7.89 (d, 2H, J = 8.5 Hz, Ar.); ^{13}C NMR (D_2O) δ 42.7 (CH_2), 122.6, 123.6, 123.8, 125.1, 132.2, 133.4, 135.2, 135.9 (Ar.), 158.7 (CN), 168.4 (CO); HRMS (ESI^+) m/z 338.1729 calcd [M^+ + H]; found 338.1734. Anal. ($C_{17}H_{21}Cl_2N_7O{\cdot}2.7H_2O$) C, H, N.

Dihydrochloride Salt of 4-Amino-*N*-(4-guanidinophenyl)-benzamide (9). Following method 2 starting from compound **11**, a white solid was obtained (95%): mp 220 °C (dec); ^1H NMR (D_2O), δ 8.10 (d, 2H, J = 7.5 Hz, Ar.), 8.17 (d, 2H, J = 7.5 Hz, Ar.), 8.23 (d, 2H, J = 7.5 Hz, Ar.), 8.42 (d, 2H, J = 7.5 Hz, Ar.); ^{13}C NMR (D_2O) δ 109.9, 117.4, 122.1, 123.3, 126.3, 128.9, 130.9, 135.8 (Ar.), 155.7 (CN), 168.0 (CO); HRMS (ESI^+) m/z 270.1355 calcd [M^+ + H]; found 270.1342. Anal. ($C_{14}H_{17}Cl_2N_5O{\cdot}1.0H_2O$) C, H, N.

Dihydrochloride Salt of 4-Amino-*N*-[4-(2-aminoimidazolino)-phenyl]benzamide (10). Following method 2 starting from compound **12**, a white solid was obtained (92%); mp 210 °C (dec); ^1H NMR (D_2O) δ 3.69 (s, 4H, CH_2), 7.25–7.31 (m, 4H, Ar.), 7.52 (d, 2H, J = 8.5 Hz, Ar.), 7.81 (d, 2H, J = 8.0 Hz, Ar.); ^{13}C NMR (D_2O) δ 42.7 (CH_2), 123.0, 123.6, 126.6, 129.2, 131.3, 131.7, 136.4, 138.9 (Ar.), 158.1 (CN), 168.4 (CO); HRMS (ESI^+) m/z 296.1511 calcd [M^+ + H]; found 296.1510. Anal. ($C_{16}H_{19}Cl_2N_5O{\cdot}1.3H_2O$) C, H, N.

Thermal Denaturation–UV Spectroscopy. Thermal denaturation experiments were conducted with a Varian Cary 300 Bio spectrophotometer equipped with a 6 × 6 multicell temperature-controlled block. Temperature was monitored with a thermistor inserted into a 1 mL quartz cuvette containing the same volume of water as in the sample cells. Absorbance changes at 260 nm were monitored from a range of 20–90 °C with a heating rate of 1 °C/min and a data collection rate of five points per °C. The salmon sperm DNA was purchased from Sigma Aldrich (extinction coefficient ε_{260} = 6600 cm^{-1} M^{-1} base). A quartz cell with a 1 cm path length was filled with a 1 mL solution of DNA polymer or DNA–compound complex. The DNA polymer (150 μM base) and the compound solution (15 μM) were prepared in a phosphate buffer [0.01 M Na_2HPO_4/NaH_2PO_4], adjusted to pH 7) so that a compound to DNA base ratio of 0.1 was obtained. The thermal denaturation temperatures of the duplex or duplex–compound complex obtained from the first derivative of the melting curves are reported.

Surface Plasmon Resonance (SPR). SPR experiments were conducted as previously described[31] with a BIAcore 2000 instrument (Biacore AB) using degassed MES buffer (10 mM 2-(*N*-morpholino)-ethanesulfonic acid, 1 mM EDTA, 92 mM NaCl, 0.0005% v/v of surfactant P20, pH 6.25) at 25 °C. The 5′-biotin labeled DNA hairpins were purchased from Midland Certified Reagent Co., Inc. (Midland, TX), with HPLC purification. The DNA hairpin sequences included 5′-biotin-CGAATTCGTCTCCGAATTCG-3′, 5′-biotin-CGTTAACGTCTCCGTTAACG-3′, and 5′-biotin-CGCGCGCGTTTTCGCGCGCG-3′, referred to in the text as AATT, TTAA, and CG, respectively. The DNA hairpins were immobilized on a streptavidin-derivatized gold chip (SA chip from BIAcore) by manual injection of a 25 nM hairpin DNA solution with a flow rate of 1 μL/min until the response units (RUs) reach about 375–415. Flow cell 1 was left blank for reference subtraction, while flow cells 2, 3, and 4 were immobilized with three different DNA hairpins. Typically, a series of different concentrations of ligand was injected onto the chip at 25 °C with a flow rate of 20 μL/min for a period of 5 min followed by a 5 min dissociation. After the dissociation process, the chip surface was regenerated with a 20 μL injection of 200 mM NaCl and 10 mM NaOH solution, injection tube rinsing, and multiple 1-min buffer injections. The observed steady–state responses, RU_{obs}, are proportional to the amount of ligand bound, and the maximum response per ligand bound (RU_{max}) was calculated as previously described.[17] The binding constants were obtained from fitting RU_{obs} vs free ligand concentration using $RU_{obs} = RU_{max}(K_1L + 2K_1K_2L^2)/(1 + K_1L + K_1K_2L^2)$ (L= ligand concentration in the flow solution).

Circular Dichroism (CD). CD spectra were collected using a JASCO J-800 spectrometer with a 1 cm cell and a scan speed of 50 nm min^{-1}. The spectra from 400 to 200 nm were averaged over six scans. A buffer baseline was collected in the same cuvette and subtracted from each of the averaged scans. The DNA concentration was 37.5 μM in base. Titrations were carried out by sequentially adding a solution of the relevant compound (0.5 mM) (with a Bp/D ratio from 22.4 to 0.56) to the buffered DNA concentration solution at 25 °C.

Isothermal Titration Calorimetry (ITC). ITC experiments were performed using a MicroCal VP-ITC instrument (MicroCal Inc., Northampton, MA) interfaced with a computer equipped with VP-2000 viewer instrument control software. ITC data were analyzed with Origin 7.0 software. In ITC experiments, an amount of 1.5 μL of 2.48 mM compound solution in 10 mM phosphate buffer was injected every 300 s for a total of 29 injections into a solution of DNA in the calorimeter cell at 2 mM. The observed heat for each injection (peak) was measured by area integration of the power peak with respect to time. ITC data were fit according to a standard model that assumes a single set of equivalent binding sites.

■ ASSOCIATED CONTENT

Ⓢ Supporting Information

Combustion analysis data of the new target compounds, cirular dichroism spectra, and atomic coordinates of the B3LYP/6-31+G*-PCM(water) optimized systems (compounds **6**, **6** plus three water molecules, **1**, and **4**). This material is available free of charge via the Internet at http://pubs.acs.org.

■ AUTHOR INFORMATION

Corresponding Author

*Phone: +353 1 896 3731. Fax: +353 1 671 2826. E-mail: rozasi@tcd.ie.

Present Addresses

[§]Departamento de Química, Universidad de La Rioja, E-26006 Logroño, Spain.

[∥]Department of Biochemistry and Molecular Biophysics, Washington University School of Medicine, St. Louis, MO, United States.

Notes

The authors declare no competing financial interest.

■ ACKNOWLEDGMENTS

This research was supported by Science Foundation Ireland (SFI-CHE275). P.S.N. thanks SFI for generous funding. F.R. thanks the Consejeria de Educacion Cultura y Deporte de la Comunidad Autonoma de La Rioja for his grant. We are indebted to Prof. Amir R. Khan (School of Biochemistry and Immunology, Trinity College Dublin, Dublin, Ireland) for providing us with access to and advice for the ITC experiments.

■ ABBREVIATIONS USED

DNA, deoxyribonucleic acid; AT, adenine–thymine base pair; HB, hydrogen bond; CD, circular dichroism; SPR, surface plasmon resonance; ITC, isothermal titration calorimetry; P/D, phosphate to drug ratio; Bp/D, base pair to drug ratio

■ REFERENCES

(1) Nagle, P. S.; Rodriguez, F.; Kahvedžić, A.; Quinn, S.; Rozas, I. *J. Med. Chem.* **2009**, *52*, 7113–7121.

(2) Nagle, P. S.; Rodriguez, F.; Quinn, S. J.; O'Donovan, D. H.; Kelly, J. M.; Nguyen, B.; Wilson, W. D.; Rozas, I. *Org. Biomol. Chem.* **2010**, *8*, 5558−5567.
(3) Rodríguez, F.; Rozas, I.; Kaiser, M.; Brun, R.; Nguyen, B.; Wilson, W. D.; García, R. N.; Dardonville, C. *J. Med. Chem.* **2008**, *51*, 909−923.
(4) Dardonville, C.; Barrett, M. P.; Brun, R.; Kaiser, M.; Tanious, F.; Wilson, W. D. *J. Med. Chem.* **2006**, *49*, 3748−3752.
(5) Motoshima, K.; Hiwasa, Y.; Yoshikawa, M.; Fujimoto, K.; Tai, A.; Kakuta, H.; Sasaki, K. *ChemMedChem* **2007**, *2*, 1527−1532.
(6) Khalaf, A. I.; Anthony, N.; Breen, D.; Donoghue, G.; Mackay, S. P.; Scott, F. J.; Suckling, C. J. *Eur. J. Med. Chem.* **2011**, *46*, 5343−5355 and references therein..
(7) Neidle, S.; Kelland, L. R.; Trent, J. O.; Simpson, I. J.; Boykin, D. W.; Kumar, A.; Wilson, W. D. *Bioorg. Med. Chem.* **1997**, *7*, 1403−1408.
(8) Liu, Y.; Kumar, A.; Depauw, S.; Nhili, R.; David-Cordonnier, M.-H.; Lee, M. P.; Ismail, M. A.; Farahat, A. A.; Say, M.; Chackal-Catoen, S.; Batista-Parra, A.; Neidle, S.; Boykin, D. W.; Wilson, W. D. *J. Am. Chem. Soc.* **2011**, *133*, 10171−10183.
(9) Mallena, S.; Lee, M. P. H; Bailly, C.; Neidle, S.; Kumar, A.; Boykin, D. W.; Wilson, W. D. *J. Am. Chem. Soc.* **2004**, *126*, 13659−13669.
(10) Munde, M.; Ismail, M. A.; Arafa, R.; Peixoto, P.; Collar, C. J.; Liu, Y.; Hu, L.; David-Cordonnier, M.-H.; Lansiaux, A.; Bailly, C.; Boykin, D. W.; Wilson, W. D. *J. Am. Chem. Soc.* **2007**, *129*, 13732−13743.
(11) Nguyen, B.; Neidle, S.; Wilson, W. D. *Acc. Chem. Res.* **2009**, *42*, 11−21.
(12) Nguyen, B.; Lee, M. P. H; Hamelberg, D.; Joubert, A.; Bailly, C.; Brun, R.; Neidle, S.; Wilson, W. D. *J. Am. Chem. Soc.* **2002**, *124*, 13680−13681.
(13) Recent reviews: (a) Kumar, V. A. *Eur. J. Org. Chem.* **2002**, 2021−2032. (b) Nielsen, P. E. *Curr. Med. Chem.* **2001**, *8*, 545−550. (c) Nielsen, P. E. *Curr. Opin. Biotechnol.* **2001**, *12*, 16−20. (d) Uhlmann, E.; Peyman, A.; Breipohl, G.; Will, D. W. *Angew. Chem., Int. Ed.* **1998**, *37*, 2796−2823. (e) Nielsen, P. E. *Acc. Chem. Res.* **1999**, *32*, 624−630.
(14) Pilch, S. D.; Poklar, N.; Gelfand, C. A.; Law, S. M.; Breslauer, K. J.; Barid, E. E.; Dervan, P. B. *Proc. Nat. Acad. Sci. U.S.A.* **1996**, *93*, 8306−8311.
(15) Lajiness, J.; Sielaff, A.; Mackay, H.; Brown, T.; Kluza, J.; Nguyen, B.; Wilson, W. D.; Lee, M.; Hartley, J. A. *Med. Chem.* **2009**, 216−226.
(16) Kahvedzic, A.; Rozas, I. Unpublished results.
(17) Dardonville, C.; Goya, P.; Rozas, I.; Alsasua, A.; Martin, I.; Borrego, M. J. *Bioorg. Med. Chem.* **2000**, *8*, 1567−1577 and references therein..
(18) (a) Rodriguez, F.; Rozas, I.; Ortega, J. E.; Meana, J. J.; Callado, L. F. *J. Med. Chem.* **2007**, *50*, 4516−4527. (b) Rodriguez, F.; Rozas, I.; Ortega, J. E.; Erdozain, A. M.; Meana, J. J.; Callado, L. F. *J. Med. Chem.* **2008**, *51*, 3304−3312. (c) Rodriguez, F.; Rozas, I.; Ortega, J. E.; Erdozain, A. M.; Meana, J. J.; Callado, L. F. *J. Med. Chem.* **2009**, *52*, 601−609.
(19) Lyng, R.; Rodger, A.; Norden, B. *Biopolymers* **1992**, *32*, 1201−1214.
(20) Rodger, A.; Norden, B. *Circular Dichroism and Linear Dichroism*; Oxford University Press: New York, 1997.
(21) (a) Nguyen, B.; Tardy, C.; Bailly, C.; Colson, P.; Houssier, C.; Kumar, A.; Boykin, D. W.; Wilson, W. D. *Biopolymers* **2002**, *63*, 281−297. (b) Liu, Y.; Kumar, A.; Boykin, D. W.; Wilson, W. D. *Biophys. Chem.* **2007**, *131*, 1−14.
(22) Buurma, N. J.; Haq, I. *Methods* **2007**, *42*, 162−172.
(23) Goodsell, D.; Dickerson, R. E. *J. Med. Chem.* **1986**, *29*, 727−733.
(24) Nagle, P. S.; Kahvedžić, A.; McCabe, T.; Rozas, I. *Struct. Chem.* **2012**, *23*, 315−323.
(25) Glass, L. S.; Nguyen, B.; Goodwin, K. D.; Dardonville, C.; Wilson, W. D.; Long, E. C.; Georgiadis, M. M. *Biochemistry* **2009**, *48*, 5943−5952.
(26) Rajendran, A.; Zhao, C.; Rajendar, B.; Thiagarajan, V.; Sato, Y.; Nishizawa, S.; Teramae, N. *Biochim. Biophys. Acta* **2010**, *1800*, 599−610.
(27) Frisch, M. J.; Trucks, G. W.; Schlegel, H. B.; Scuseria, G. E.; Robb, M. A.; Cheeseman, J. R.; Scalmani, G.; Barone, V.; Mennucci, B.; Petersson, G. A.; Nakatsuji, H.; Caricato, M.; Li, X.; Hratchian, H. P.; Izmaylov, A. F.; Bloino, J.; Zheng, G.; Sonnenberg, J. L.; Hada, M.; Ehara, M.; Toyota, K.; Fukuda, R.; Hasegawa, J.; Ishida, M.; Nakajima, T.; Honda, Y.; Kitao, O.; Nakai, H.; Vreven, T.; Montgomery, J. A., Jr.; Peralta, J. E.; Ogliaro, F.; Bearpark, M.; Heyd, J. J.; Brothers, E.; Kudin, K. N.; Staroverov, V. N.; Kobayashi, R.; Normand, J.; Raghavachari, K.; Rendell, A.; Burant, J. C.; Iyengar, S. S.; Tomasi, J.; Cossi, M.; Rega, N.; Millam, J. M.; Klene, M.; Knox, J. E.; Cross, J. B.; Bakken, V.; Adamo, C.; Jaramillo, J.; Gomperts, R.; Stratmann, R. E.; Yazyev, O.; Austin, A. J.; Cammi, R.; Pomelli, C.; Ochterski, J. W.; Martin, R. L.; Morokuma, K.; Zakrzewski, V. G.; Voth, G. A.; Salvador, P.; Dannenberg, J. J.; Dapprich, S.; Daniels, A. D.; Farkas, Ö.; Foresman, J. B.; Ortiz, J. V.; Cioslowski, J.; Fox, D. J. *Gaussian 09*, revision A.1; Gaussian, Inc.: Wallingford, CT, 2009.
(28) (a) Becke, A. D. *J. Chem. Phys.* **1993**, *98*, 5648−5652. (b) Lee, C.; Yang, W.; Parr, R. G. *Phys. Rev. B* **1988**, *37*, 785−789.
(29) Frisch, M. J.; Pople, J. A.; Binkley, J. S. *J. Chem. Phys.* **1984**, *80*, 3265−3269.
(30) Bader, R. F. W. *Atoms in Molecules: A Quantum Theory*; Clarendon Press: Oxford, U.K., 1990.
(31) (a) Nguyen, B.; Tanious, F. A.; Wilson, W. D. *Methods* **2007**, *42*, 150−161. (b) Tanious, F. A.; Nguyen, B.; Wilson, W. D. *Methods Cell Biol.* **2008**, *84*, 53−77.